| | |
|---|---|
| **Titre:** Title: | Comparison of two-dimensional flood propagation models: SRH-2D and Hydro_AS-2D |
| **Auteurs:** Authors: | Basile Lavoie, & Tew-Fik Mahdi |
| **Date:** | 2017 |
| **Type:** | Article de revue / Article |
| **Référence:** Citation: | Lavoie, B., & Mahdi, T.-F. (2017). Comparison of two-dimensional flood propagation models: SRH-2D and Hydro_AS-2D. Natural Hazards, 86(3), 1207-1222. https://doi.org/10.1007/s11069-016-2737-7 |



**Document publié chez l'éditeur officiel**
Document issued by the official publisher

| | |
|---|---|
| **Titre de la revue:** Journal Title: | Natural Hazards (vol. 86, no. 3) |
| **Maison d'édition:** Publisher: | Springer |
| **URL officiel:** Official URL: | https://doi.org/10.1007/s11069-016-2737-7 |
| **Mention légale:** Legal notice: | This is a post-peer-review, pre-copyedit version of an article published in Natural Hazards (vol. 86, no. 3) . The final authenticated version is available online at: https://doi.org/10.1007/s11069-016-2737-7 |

# Comparison of two-dimensional Flood Propagation Models: SRH-2D and Hydro_AS-2D

Basile Lavoie[1], Tew-Fik Mahdi Ph.D.[2]

[1]Département des génies Civil, Géologique et des Mines (CGM), École Polytechnique de Montréal, C.P. 6079, succursale Centre-Ville, Montréal, QC H3C 3A7, Canada. Email: basile.lavoie@polymtl.ca

[2] Professor, Département des génies Civil, Géologique et des Mines (CGM), École Polytechnique de Montréal, C.P. 6079, succursale Centre-Ville, Montréal, QC H3C 3A7, Canada (Corresponding author). Email: tewfik.mahdi@polymtl.ca. Phone: (514) 340-4711 Ext.: 5874. Fax: (514) 340-4191

## Abstract

This article presents a comparison between two two-dimensional finite volume flood propagation models: SRH-2D and Hydro_AS-2D. The models are compared using an experimental dam-break test-case provided by Soares-Frazão (2007). Four progressively refined meshes are used, and both models react adequately to mesh and time step refinement. Hydro_AS-2D shows some unphysical oscillations with the finest mesh and a certain loss of accuracy. For that test-case, Hydro_AS-2D is more accurate for all meshes and generally faster than SRH-2D. Hydro_AS-2D reacts well to automatic calibration with PEST, whereas SRH-2D has some difficulties in retrieving the suggested Manning's roughness coefficient.

**Author Keywords:** Model comparison; Two-dimensional flow modeling; Hydro_AS-2D; SRH-2D; Automatic calibration

## Notations

| | |
|---|---|
| D | Hydraulic diameter |
| e | Source term |
| g | Gravitational acceleration |
| h | Water depth |
| k | Turbulent kinetic energy |
| n | Manning's roughness coefficient |
| $S_{fx}$, $S_{fy}$ | Energy slope |
| $S_{bx}$, $S_{by}$ | Bed slope |
| T | Turbulence stress |
| u, v | Velocity components |
| z | Water surface elevation |
| $z_b$ | Bed elevation |
| $\mu$ | Eddy viscosity |
| $\mu_0$ | Kinematic viscosity of water |
| $\mu_t$ | Turbulent eddy viscosity |
| $\rho$ | Mass density |
| $\tau$ | Shear stress |

# 1 Introduction

Flood propagation may induce important human and material losses and remains a major challenge for hydraulic engineers due to the complexity of the phenomenon and therefore to the difficulties that arise in their numerical modeling. Two-dimensional models are now widely used in flood propagation modeling owing to the gain in precision they offer and their relatively small time consumption. Different types of methods were used for the numerical modeling of shallow water equations as finite differences, finite elements and finite volumes. For fluid flows, the last is currently accepted as the most accurate and has been implemented in several models such as TUFLOW-FV (BMTWBM 2014), RiverFlow2D (Hydronia 2015), SRH-2D (Lai 2008), Hydro_AS-2D (Nujic 2003), HEC-RAS (Brunner 2016) and BASEMENT (Vetsch 2015). If these models are usually validated by their designer, few model-to-model comparisons exist. It is yet of great importance for practicing engineers to have objective and precise comparisons on which they can rely for the choice of a flood propagation model. The aim of this paper is to provide such a comparison for two models: Hydro_AS-2D, which is mainly used in European countries, and SRH-2D, largely used in North America.

SRH-2D was validated against numerous experimental, analytical and river cases. Lai (2008) and Lai (2010) showed that the model reacts correctly compared with the analytical solution of a transcritical flow with a hydraulic jump in a 1D channel that was proposed by MacDonald (1996). SRH-2D was also used to model the 2D diversion flow case measured by Shettar et Murthy (1996) with the conclusion that the flow was better modeled along the walls by SRH-2D with the k-epsilon turbulence model than with the parabolic model (Lai 2008; Lai 2010). Experimental data of a channel with bend proposed by Zarrati et al. (2005) were modeled with SRH-2D and showed that the computed water depth was less sensitive to mesh resolution than the velocity (Lai 2008; Lai 2010). The model was used to evaluate the impact of a dam removal on the Sandy River Delta with satisfactory results. A similar study was undertaken for the Savage Rapids dam removal and achieved good results in modeling the water depth and hydraulic jump (Lai 2008; Lai 2010).

Jones (2011) made a comparison of four two-dimensional hydrodynamic models: ADH (Berger et al. 2013), FESWMS (Froehlich 2002), RMA2 (Donnell 2006) and Hydro_AS-2D (Nujic 2003). Applied to three test-cases, Hydro_AS-2D proved to be the most stable and easy to use and was able to run in some cases where other models could not. Hydro_AS_2D was also the fastest model.

Tolossa (2008) and Tolossa et al. (2009) compared the two-dimensional hydrodynamic models Hydro_AS-2D and SRH-W, which was the first released version of SRH-2D. The models were compared on three river reaches and were able to appropriately recreate the water depth. The authors report that SRH-W seems more sensitive to mesh refinement, meaning that a finer mesh was needed to reach a precision comparable to Hydro_AS-2D. SRH-W was the fastest model of this study.

Both models have been tested in numerous studies and have been proven to be reliable. However, the previous comparisons and test-cases did not state which of SRH-2D and Hydro_AS-2D could best predict the water depth. It is therefore the purpose of this paper to provide a clear statement on which model is best for forecasting flow parameters. The computation time will be compared as well to confirm or nuance previous studies. In addition, a new feature, which has, to the best of our knowledge, never been used to compare hydrodynamic models, is studied for the purpose of this comparison: automatic calibration. Automatic calibration is becoming increasingly used in hydrodynamic and hydrologic modeling (Ellis et al. 2009; Fabio et al. 2010; McCloskey et al. 2011; McKibbon et Mahdi 2010) because it provides important gains not only in the calibration's necessary time but also in the calibrated parameters' values. Thus, it is important to ensure that models react correctly to an automatic calibration.

# 2 Presentation of Models

## 2.1 SRH-2D Version 3

SRH-2D solves the shallow water equations using the following form (Lai 2008; Lai 2010):

$$\frac{\partial h}{\partial t} + \frac{\partial hu}{\partial x} + \frac{\partial hv}{\partial y} = e \qquad \text{(Eq. 1)}$$

$$\frac{\partial hu}{\partial t} + \frac{\partial huu}{\partial x} + \frac{\partial hvu}{\partial y} = \frac{\partial hT_{xx}}{\partial x} + \frac{\partial hT_{xy}}{\partial y} - gh\frac{\partial z}{\partial x} - \frac{\tau_{bx}}{\rho} \qquad \text{(Eq. 2)}$$

$$\frac{\partial hv}{\partial t} + \frac{\partial huv}{\partial x} + \frac{\partial hvv}{\partial y} = \frac{\partial hT_{xy}}{\partial x} + \frac{\partial hT_{yy}}{\partial y} - gh\frac{\partial z}{\partial y} - \frac{\tau_{by}}{\rho} \qquad \text{(Eq.3)}$$

The friction is determined using the Manning equation:

$$\begin{pmatrix}\tau_{bx}\\ \tau_{by}\end{pmatrix} = \rho C_f \begin{pmatrix}u\\ v\end{pmatrix}\sqrt{u^2+v^2} \qquad C_f = \frac{gn^2}{h^{1/3}} \qquad \text{(Eqs. 4 and 5)}$$

Boussinesq equations are used to compute the turbulence stresses:

$$T_{xx} = 2(\mu_0+\mu_t)\frac{\partial u}{\partial x} - \frac{2}{3}k \qquad \text{(Eq. 6)}$$

$$T_{xy} = (\mu_0+\mu_t)\left(\frac{\partial u}{\partial y}+\frac{\partial v}{\partial x}\right) \qquad \text{(Eq. 7)}$$

$$T_{yy} = 2(\mu_0+\mu_t)\frac{\partial v}{\partial y} - \frac{2}{3}k \qquad \text{(Eq. 8)}$$

where h is the water depth, u and v are the velocity components, z is the water surface elevation, e is a source term, T are the turbulent stresses, τ is the shear stress, g is the gravitational acceleration, ρ is the mass density, $\mu_0$ is the kinematic viscosity of water, $\mu_t$ is the turbulent eddy viscosity, k is the turbulent kinetic energy, and n is Manning's roughness coefficient.

SRH-2D proposes two turbulence models: k-epsilon and depth-averaged parabolic models. The parabolic model is used in the present study because it is the only turbulence model used by Hydro_AS-2D, and a proper comparison necessitates identical parameters. SRH-2D uses a wetting–drying front limit of 0.001 m. Below this value, water depth is considered to be equal to 0 m on the cell, and SRH-2D does not solve the shallow water equations (Lai 2010).

## 2.2 Hydro_AS-2D Version 4

Shallow water equations, as solved by Hydro_AS-2D, are expressed in vectors (Nujic 2003):

$$\frac{\partial w}{\partial t}+\frac{\partial f}{\partial x}+\frac{\partial g}{\partial y}+S=0 \quad \text{(Eq. 9)}$$

$$w = \begin{bmatrix} z \\ uh \\ vh \end{bmatrix} \qquad f = \begin{bmatrix} uh \\ u^2h + 0.5gh^2 + \mu h \frac{\partial u}{\partial x} \\ uvh - \mu h \frac{\partial v}{\partial x} \end{bmatrix} \quad \text{(Eq. 10)}$$

$$g = \begin{bmatrix} vh \\ uvh - \mu h \frac{\partial u}{\partial y} \\ v^2h + 0.5gh^2 + \mu h \frac{\partial v}{\partial y} \end{bmatrix} \quad S = \begin{bmatrix} 0 \\ gh(S_{fx} - S_{bx}) \\ gh(S_{fy} - S_{by}) \end{bmatrix} \quad \text{(Eq. 11)}$$

The bed slope is defined as follows:

$$S_{bx} = -\frac{\partial z_b}{\partial x} \qquad S_{by} = -\frac{\partial z_b}{\partial y} \quad \text{(Eqs. 12 and 13)}$$

The energy slope is computed following the Darcy–Weisbach equation, and the friction coefficient is determined with the Manning formula:

$$S_f = \left(6.34 \frac{2gn^2}{D^{1/3}}\right) \cdot \left(\frac{v|v|}{2gD}\right) \qquad \text{(Eq. 14)}$$

where μ represents the eddy viscosity, $S_f$ is the energy slope, $z_b$ is the bed elevation, and D is the hydraulic diameter.

The default wetting–drying front limit is set to 0.01 m but is lowered to 0.001 m for the current study. Time steps are calculated automatically and continuously by Hydro_AS-2D over the modeling.

## 2.3 SMS Version 12.1

The Surface–water Modeling System, SMS (AQUAVEO 2016), facilitates the required pretreatment and post-treatment for hydraulic modeling of open channel flow. SMS includes many characteristics of GIS software and uses them, for example, in the creation of quality meshes. The results may be viewed in three dimensions, and many tools are available for their treatment, which makes SMS very versatile and usable with multiple models (AQUAVEO 2016). For the present study, SMS allows with great ease the use of the same mesh and boundary conditions for the two models, SRH-2D and Hydro_AS-2D, which is necessary for a proper comparison.

## 2.4 PEST Version 13

PEST (Doherty 2005) is a software program that executes the automatic calibration and sensibility analysis of any model based on input and output files. In this study, only the automatic calibration module is used. Automatic calibration with PEST requires three main types of files: template, instruction and control files (figure 1).

- Template files act as models for PEST when creating input files to calibrate the model (i.e., SRH-2D and Hydro_AS-2D).
- Instruction files aid PEST in the interpretation of the model's output by indicating the values that should be used for the calibration.
- The control file contains calibration instructions, such as stopping criteria and observed values. It relates the template and instruction files to the model's files to which they refer.

PEST is therefore model independent and relatively simple to use, which makes it a powerful tool for the calibration of two-dimensional hydrodynamic models.

# 3 Methodology

The comparison of SRH-2D and Hydro_AS-2D is made on experimental data and aims to verify the accuracy of both models, their sensitivity to spatial and time discretization, and their response to automatic calibration.

## 3.1 Test-case

The two models are compared using an experimental dataset presented by Soares-Frazão (2007) in which a dam break wave over a triangular bottom sill is studied. The rectangular channel has a width of 0.5 m and a length of 5.6 m, and the sill height is 0.065 m with a symmetrical slope of approximatively 14% (figure 2). The suggested Manning's roughness coefficient is 0.011 s/m$^{1/3}$. The initial conditions (figure 2) are made of an upstream reservoir in which the water depth is 0.111 m and by a downstream pool, isolated from the rest of the channel by the sill, with a water depth of 0.02 m. The central section is initially dry. The reservoir is isolated by a gate whose sudden removal creates the propagation of the dam-break wave upon the channel.

All four boundaries of the channel consist of walls, meaning that the wave will successively reflect against the downstream and upstream walls. The wave first propagates on the dry bed to reach the sill where the water is partly reflected to the upstream part of the channel and partly continues to reach the water pool located downstream of the sill. Reflections are then simultaneously observed in the sections of the channel located on both sides of the sill.

Three gauges are positioned around the triangular sill to monitor the incidence of this feature on the flow. The monitoring lasts 45 s, during which the water depths are available every 0.01 s, for a total of 4501 measurements for each gauge.

## 3.2 Time Step and Mesh Sensitivity and Water Depth Accuracy

The simulation is made with SRH-2D on four progressively refined meshes (figure 3) that are all modeled with five time steps (tables 1 and 2). These twenty simulations are then used to investigate the sensitivity of SRH-2D to these parameters and will ensure that a mesh and time step independent solution is achieved. The time step providing the best results is afterward used for the comparison with Hydro_AS-2D. Hydro_AS-2D computes the time step required to fulfill the Courant condition, so the user does not have influence on that parameter. Therefore, only the mesh sensitivity is evaluated for this model. The meshes used are the same as those presented above for SRH-2D.

The comparison is then made on the four meshes, and the quality of the simulations is quantified through the calculation of the root mean squared error (RMSE) considering the calculated and measured water depth every 0.1 s for a total of 450 benchmark measurements by gauge.

All simulations last 45 s, and the depth-averaged parabolic model is used for turbulence for both SRH-2D and Hydro_AS-2D. The minimum water depth for the treatment of the wetting and drying front is 0.001 m, and the maximum velocity is 15 m/s for Hydro_AS-2D. The wetting and drying front limit is also 0.001 m for SRH-2D, but the maximum velocity is unknown. All wall boundaries are assigned a no-slip condition. All calculations are made with a 64 GB server with an Intel Xeon CPU E5-2630 v3 @2.40 GHz processor.

## 3.3 Response to Automatic Calibration

The dam-break models, using SRH-2D and Hydro_AS-2D, are automatically calibrated with PEST to verify whether they can properly retrieve the Manning's roughness coefficient suggested by Soares-Frazão (2007) and the incidence of that calibration on the water depth RMSE.

The automatic calibration requires experimental measurements to compare the simulations and choose the best Manning's coefficient. Because the calibration time increases proportionally to the number of measurements, all available measurements cannot be used. The number of benchmark values is therefore set to 27, meaning one measurement at each gauge every 5 s. The coarsest mesh is used for the calibration, and Manning's roughness coefficient is allowed to vary between 0.005 s/m$^{1/3}$ and 0.05 s/m$^{1/3}$ for both SRH-2D and Hydro_AS-2D.

# 4 Results and Discussion

## 4.1 Time Step and Mesh Sensitivity—SRH-2D

Figure 4 presents the evolution of RMSE relative to time step refinement for each gauge and each mesh and shows a quick stabilization of the RMSE for the coarsest mesh, whereas the finest mesh has a drastic reduction of its error between the first and fourth time steps (ex: from 0.0182 m to 0.0092 m for gauge 3). The error is insignificantly modified between the fourth and fifth time steps (from 0.0092 m to 0.0087 m for gauge 3); these solutions can then be considered to have reached time step independence.

The fifth time step gives the best solution for all meshes. It is used to compute the evolution of water depth RMSE relative to mesh refinement, which can be observed in figure 5, and diminishes with the mesh density (from 0.0094 m to 0.0087 m for gauge 3).

These results conform to theory because the time step needed to ensure stability, and convergence is reduced proportionally to the grid size. SRH-2D has a good response to time step and mesh density refinement.

## 4.2 Mesh Sensitivity—Hydro_AS-2D

Hydro_AS-2D continuously adjusts the time step during the simulation to ensure numerical stability. Therefore, only the mesh sensitivity is addressed. Figure 6 shows a global reduction of RMSE following the mesh refinement with the exception of gauges 1 and 3, which present a slight increase for the fourth mesh (0.0004 m for gauge 1 and 0.0001 m for gauge 3). Similar results were published by Družeta et al. (2009) and Boz et al. (2014), who respectively investigated the influence of mesh density on the resolution of shallow water equations with the Q-scheme and the MUSCL–Hancock scheme and on the resolution of the Navier–Stokes equations with the CFD code ANSYS CFX.

## 4.3 Water Depth Profiles and Oscillations

Figure 7 shows the evolution of water depth in time for all meshes at gauge 1 as calculated by Hydro_AS-2D. The mesh refinement greatly benefits the results for the first 15 s of the simulation where the experimental and computed water depths become very similar. However, the refinement seems to increase the oscillation amplitude beyond the $15^{th}$ second. These oscillations are not physically representative when compared to the experimental line. This phenomenon may also be noted at a smaller scale for gauge 2 but is absent at gauge 3, which may be because these oscillations are induced by the wall reflection. This phenomenon was also noted by Družeta et al. (2009), who observed that the oscillation amplitude was increasing with increasing mesh refinement but observed no dependence between the oscillation frequency and the mesh density, which is not the case of the current study in which lower spatial resolution seems to yield a higher oscillation frequency (figure 7).

SRH-2D has its general water depth results greatly improved by the mesh refinement, whereas the experimental and computed depths become closer (figure 8). The augmented spatial resolution also gives a better representation of the oscillations. Moreover, these oscillations are offset in time but stay physically consistent with the experimental data unlike Hydro_AS-2D.

Comparing figures 7 and 8, Hydro_AS-2D seems to provide a better fit with the experimental data for all meshes, especially for the first 15 s.

## 4.4 Water Depth RMSE

Figure 9 shows a comparison of computed water depth RMSEs for SRH-2D and Hydro_AS-2D with all four meshes. The smallest time step is used for all SRH-2D simulations because it provides the best results. For all meshes, Hydro_AS-2D is more accurate at all gauges and all meshes, and the most important difference between the two models' RMSE is observed at the third gauge (0.0094 m for SRH-2D versus 0.0038 m for Hydro_AS-2D with the coarsest mesh). SRH-2D has its largest error at gauge 3, which is initially dry and may represent the difficulty of modeling the wave propagation on a dry bed. This was noted as a current difficulty in numerical modeling by Soares-Frazão (2007) and was one of the main purposes of the experiment used in the current study. Hydro_AS-2D shows the most important error at gauge 2, which is placed after the downstream side of the sill. This may be because the important slope of the sill creates a flow that is not fully 2D and is therefore more difficult to represent by the model.

## 4.5 Computation time

Computation time is highly related to the number of mesh elements and time steps. Only mesh density influence is studied for Hydro_AS-2D because the model automatically adjusts the time step. SRH-2D gives full control of these two parameters, so both mesh density and time step sensitivity are considered.

Figure 10 shows the evolution of computation time relative to the time step of all meshes for SRH-2D. The computation time increases with increasing mesh and time step resolutions. There is a dramatic increase in the computational time for time step 5 (0.0001 s) compared with time step 4 (0.0004 s), especially for the finest mesh (11.6 h versus 39.1 h).

Because the time step has such a drastic influence on the computation time, this parameter must be properly chosen to form a reliable comparison and avoid the use of a very small time step that would unnecessarily increase the computation time. Therefore, the chosen time step for SRH-2D is the one allowing time step independence of the model and is selected based on the results of figure 4 (section *Time Step and Mesh Sensitivity*). Table 3 summarizes the time step used for the two models in the computation time comparison. The computation times are pretty much equal for the first mesh, but Hydro_AS-2D is generally faster by an average factor of 7.51 h/h (figure 11). One should note that the largest difference is observed for the finest mesh where Hydro_AS-2D is 15.8 times faster, whereas the time step is almost the same for both models ($\Delta t_{SRH\text{-}2D}$=0.0004 s and $\Delta t_{HYDRO\_AS\text{-}2D}$=0.00037 s). The capacity of Hydro_AS-2D to parallelize the calculation can explain this difference between the two models. The code structures may also impact the computation time, but this information is not available for these models.

## 4.6 Response to Calibration

Table 4 summarizes the results and parameters of the automatic calibrations with PEST for the two models. SRH-2D necessitates 10 iterations and 38 model calls, whereas Hydro_AS-2D completes the calibration in 3 iterations and 19 model calls. SRH-2D is slightly faster (1.08 h versus 1.2 h), which is not surprising considering that this model has been shown to be faster for the coarsest mesh, the only mesh used for the automatic calibration, when used with a time step of 0.005 s (see section *Computation Time*).

Automatic calibration with Hydro_AS-2D provides Manning's roughness coefficient of 0.0096 s/m$^{1/3}$, which is very similar to 0.011 s/m$^{1/3}$ as suggested by Soares-Frazão (2007). SRH-2D, when calibrated, gives a very different value of 0.0219 s/m$^{1/3}$. Hydro_AS-2D provides very similar RMSEs with calibrated and suggested Manning's roughness coefficients; the maximal difference is 0.0003 m, which is observed at gauge 3. This is consistent with the fact that the calibrated

Manning's coefficient is very close to the suggested coefficient. Therefore, Hydro_AS-2D has a good response to automatic calibration. When calibrated, SRH-2D shows a greater improvement of its RMSE, which decreases by up to 0.0032 m at gauge 2. If only the water depth RMSE is considered to qualify the automatic calibration, SRH-2D seems to be benefiting from a Manning's roughness coefficient that is approximatively twice the suggested coefficient. This is unlikely because that parameter would lose its physical representativeness of the actual channel's roughness. This is confirmed by the observation of the evolution of water depth in time at gauge 1 (figure 12). The calibrated computed water depth becomes closer to the experimental water depth in the second half of the experiment; however, it is clear that the shape of oscillation is lost with the calibration and is better represented by the original suggested Manning's coefficient. Despite the reduced water depth RMSE, the automatic calibration is unsuitable for SRH-2D in that case. One can note that Hydro_AS-2D remains generally more accurate than SRH-2D, the only exception being gauge 2 at which SRH-2D gives a smaller RMSE.

# 5 Conclusion

Two flood propagation models, Hydro_AS-2D and SRH-2D, were compared in terms of their capacity to properly model an experimental dam-break test case. The two models were shown to have a good response to mesh and time step refinement; however, Hydro_AS-2D showed unphysical oscillations and an increase in the water depth RMSE at two of the three gauges with the finest mesh. These observations support the idea that too much spatial resolution could negatively affect the accuracy of a model as noted by Družeta et al. (2009) and Boz et al. (2014). Hydro_AS-2D computed lower RMSEs for all meshes and was therefore more accurate than SRH-2D. Hydro_AS-2D was up to 15.8 times faster than SRH-2D. This contrasts with the results of Tolossa (2008) and Tolossa et al. (2009), who found that SRH-W (the previous version of SRH-2D) was faster than Hydro_AS-2D. Hydro_AS-2D responded well to the automatic calibration of Manning's roughness coefficient by computing a coefficient very similar to the suggested one, whereas SRH-2D computed a very different coefficient that lowered the water depth RMSE but with no physical representativeness of the actual channel.

This research has exposed some of the differences between two major hydrodynamic models and clarified their respective assets to offer an objective point of comparison that will be helpful for industrial and research engineers in choosing a modeling tool for flood propagation.

## Acknowledgments

This research was supported in part by a National Science and Engineering Research Council (NSERC) Discovery Grant, application No: RGPIN-2016-06413.

## References

AQUAVEO (2016). "SMS 12.1 - The Complete Surface-water Solution." <http://www.aquaveo.com/software/sms-surface-water-modeling-system-introduction>. (March 10, 2016).

Berger, R. C., Tate, J. N., Brown, G. L., et Savant, G. (2013). "Adaptive Hydraulics Users Manual." Coastal and Hydraulics Laboratory Engineer Research and Development Center, 99.

BMTWBM (2014). "TUFLOW FV User Manual." *Flexible Mesh Modelling*, BMT WBM, Brisbane, Australia, 183.

Boz, Z., Erdogdu, F., et Tutar, M. (2014). "Effects of mesh refinement, time step size and numerical scheme on the computational modeling of temperature evolution during natural-convection heating." *Journal of Food Engineering*, 8-16.

Brunner, G. W. (2016). "HEC-RAS River Analysis System User's Manual." US Army Corps of Engineers, Davis, CA, USA, 960.

Doherty (2005). "PEST, Model-Independant Parameter Estimation, USer Manual: 5th Edition." Watermark Numerical Computing.

Donnell, B. P. (2006). "RMA2 WES Version 4.5." I. King, J. V. Letter, W. H. McAnally, et W. A. Thomas, eds., US Army, Engineer Research and Development Center, 277.

Družeta, S., Sopta, L., Maćešić, S., et Črnjarić-Žic, N. (2009). "Investigation of the Importance of Spatial Resolution for Two-Dimensional Shallow-Water Model Accuracy." *Journal of Hydraulic Engineering*, 917-925.

Ellis, R. J. l., Doherty, J., Searle, R. D., et Moodie, K. (2009). "Applying PEST (Parameter ESTimation) to improve parameter estimation and uncertainty analysis in WaterCAST

models." *18th World IMACS/MODSIM Congress*, Modelling and Simulation Society of Australia and New-Zealand Inc., 3158-3164.
Fabio, P., Aronica, G. T., et Apel, H. (2010). "Towards automatic calibration of 2-D flood propagation models." *Hydrology and Earth System Sciences*, 10.5194/hess-14-911-2010, 911-924.
Froehlich, D. C. (2002). "User's Manual for FESWMS FST2DH." Federal Highway Administration, 209.
Hydronia (2015). "RiverFlow2D Plus Two-Dimensional Finite-Volume River Dynamics Model." Hydronia, Pembroke Pines, FL, USA, 157.
Jones, D. A. (2011). "The Transition from Earlier Hydrodynamic Models to Current Generation Models." Master of Science, Brigham Young University, Brigham.
Lai, Y. G. (2008). "SRH-2D version 2: Theory and User's Manual." U.S. Department of the interior - Bureau of Reclamation, Denver.
Lai, Y. G. (2010). "Two-Dimensional Depth-Averaged Flow Modeling with an Unstructured Hybrid Mesh." *Journal of Hydraulic Engineering*, 12-23.
Lin, Z. (2010). "Getting Started with PEST." The University of Georgia, Athens, GA.
MacDonald, I. (1996). "Analysis and Computation of Steady Open Channel Flow." Doctor of Philosophy, University of Reading, Reading, UK.
McCloskey, G. L. l. E., R.J., Waters, D. K., et Stewart, J. (2011). "PEST hydrology calibration process for source catchments - applied to the Great Barrier Reef, Quennsland." *19th International Congress on Modelling and Simulation*, Modelling and Simulation Society of Australia and New-Zealand Inc., 2359-2366.
McKibbon, J., et Mahdi, T.-F. (2010). "Automatic Calibration Tool for River Models Based on the MHYSER Software." *Natural Hazards*, 54(3), 879-899.
Nujic, M. (2003). "Hydro_AS-2D A Two-Dimensional Flow Model For Water Mangement Applications User's Manual."Rosenheim, Deutschland.
Shettar, A. S., et Murthy, K. K. (1996). "A numerical Study of Division of Flow in Open Channels." *Journal of Hydraulic Research*, 34(5), 651-675.
Soares-Frazão, S. (2007). "Experiments of dam-break wave over a triangular bottom sill." *Journal of Hydraulic Research*, 10.1080/00221686.2007.9521829, 19-26.
Tolossa, G. H. (2008). "Comparison of 2D Hydrodynamic models in River Reaches of Ecological Importance:Hydro_AS-2D and SRH-W." Institut für Wasserbau, Universität Stuttgart, Stuttgart.
Tolossa, H. G., Tuhtan, J., Schneider, M., et Wieprecht, S. "Comparison of 2D Hydrodynamic Models in River Reaches of Ecological Importance Hydro_AS-2D and SRH-W." *Proc., 33rd IAHR World Congress*, 604-611.
Vetsch, D. (2015). "System Manuls of Basement." Swiss Federal Institute of Technology Zurich, Zurich, 178.
Zarrati, A. R., Tamai, N., et Jin, Y. C. (2005). "Mathematical Modeling of Meandering Channels with a Generalized Depth Averaged Model." *Journal of Hydraulic Engineering*, 131(6), 467-475.

# Figure Captions

**Fig. 1.** Automatic calibration with PEST – Adapted from Lin (2010)

**Fig. 2.** Channel geometry, initial conditions and gauges positions

**Fig. 3.** Meshes (0.5 m × 0.45 m zone)

**Fig. 4.** Water depth RMSE relative to time step refinement at Gauges 1-3—SRH-2D

**Fig. 5.** Water depth RMSE relative to mesh refinement—SRH-2D

**Fig. 6.** Water depth RMSE relative to mesh refinement—Hydro_AS-2D

**Fig. 7.** Water depth at gauge 1 for meshes 1-4—Hydro_AS-2D

**Fig. 8.** Water depth at gauge 1 for meshes 1-4—SRH-2D

**Fig. 9.** Comparison of computed water depth RMSEs—Meshes 1-4

**Fig. 10.** Computation time relative to time step refinement—SRH-2D

**Fig. 11.** Comparison of computation time

**Fig. 12.** Comparison of water depth with suggested and calibrated Manning's coefficients at gauge 1—SRH-2D

# Table Captions

**Table 1.** Time steps

**Table 2.** Meshes

**Table 3.** Time steps used for computation time comparison

**Table 4.** Calibration parameters and results

Figure 1



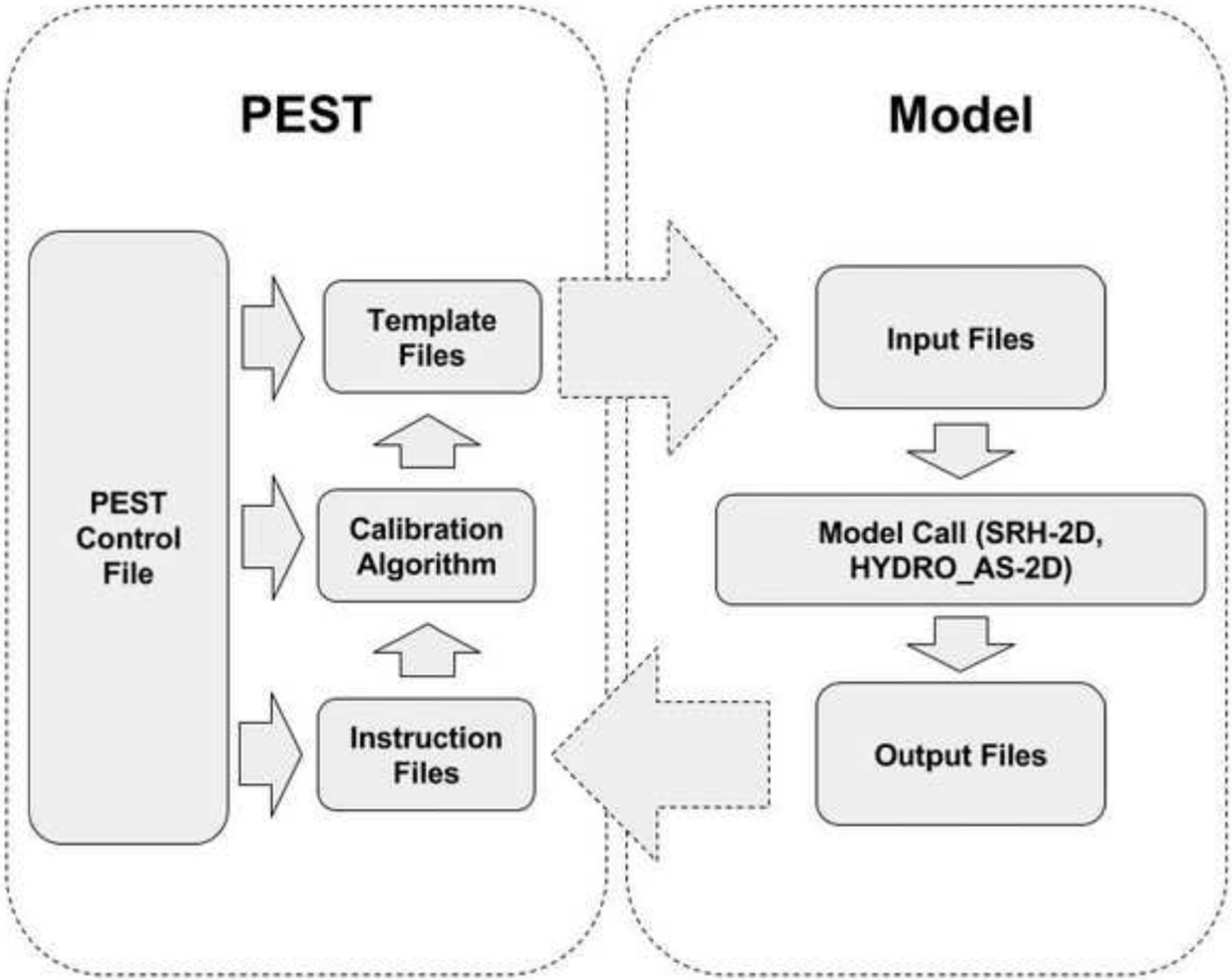
PEST
Model
PEST Control File
Template Files
Calibration Algorithm
Instruction Files
Input Files
Model Call (SRH-2D, HYDRO_AS-2D)
Output Files

Figure 2



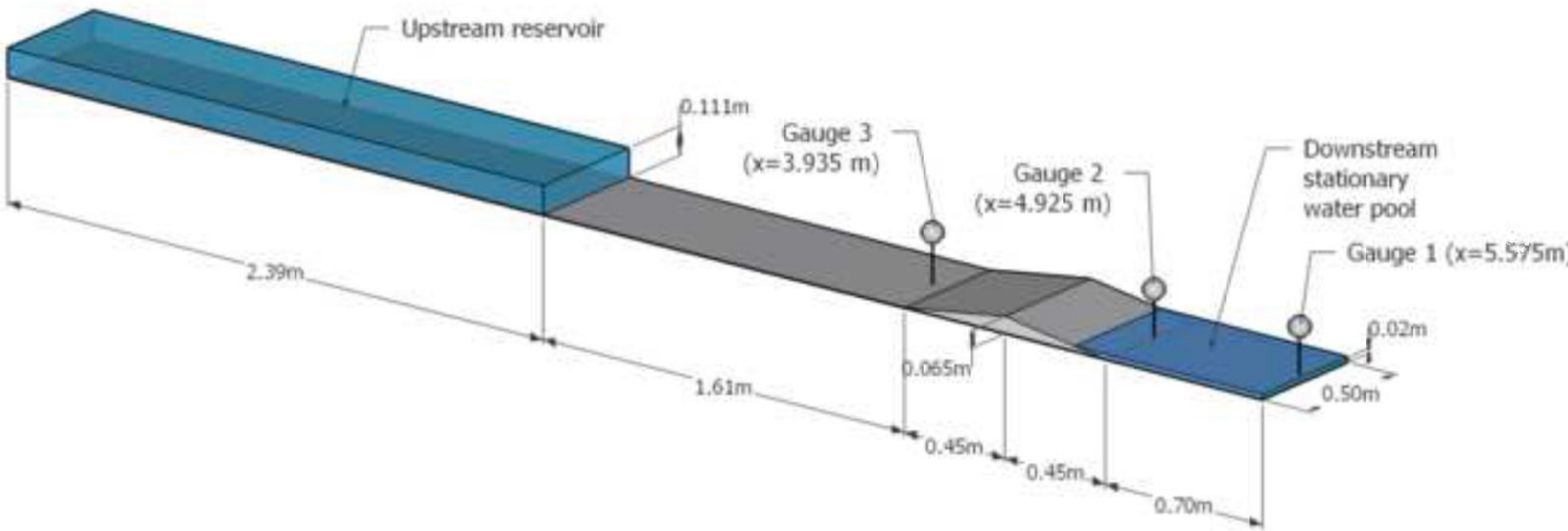

Upstream reservoir
0.111m
Gauge 3
(x=3.935 m)
Gauge 2
(x=4.925 m)
Downstream
stationary
water pool
Gauge 1 (x=5.575m)
0.02m
0.50m
2.39m
1.61m
0.065m
0.45m
0.45m
0.70m

Figure 3



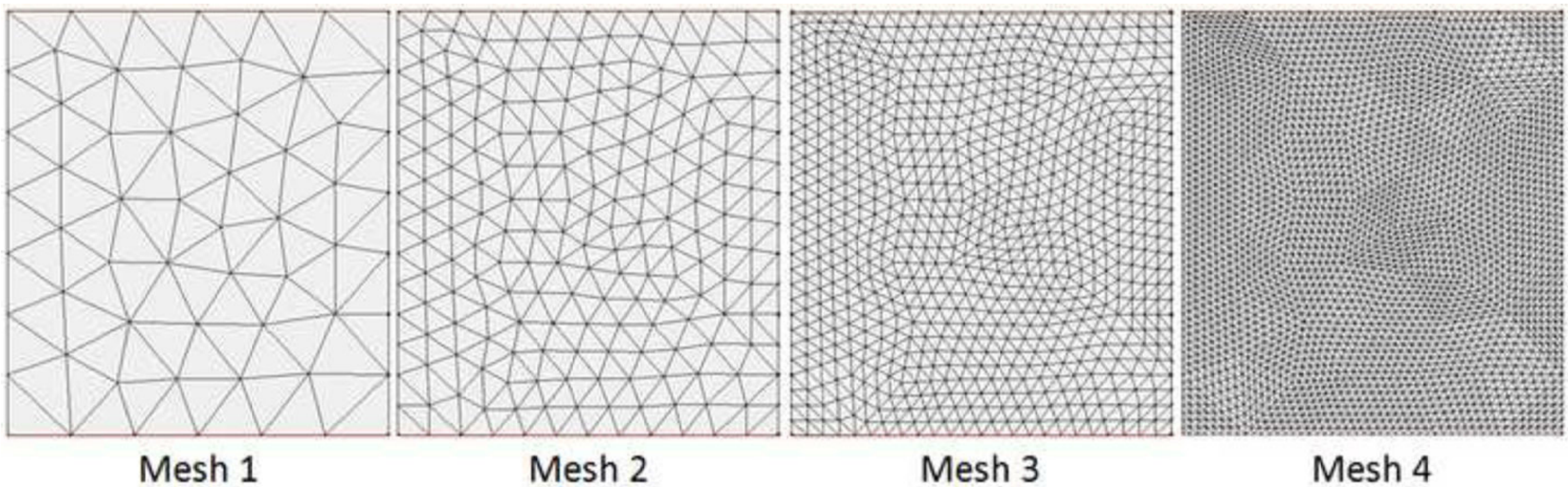

Figure 4



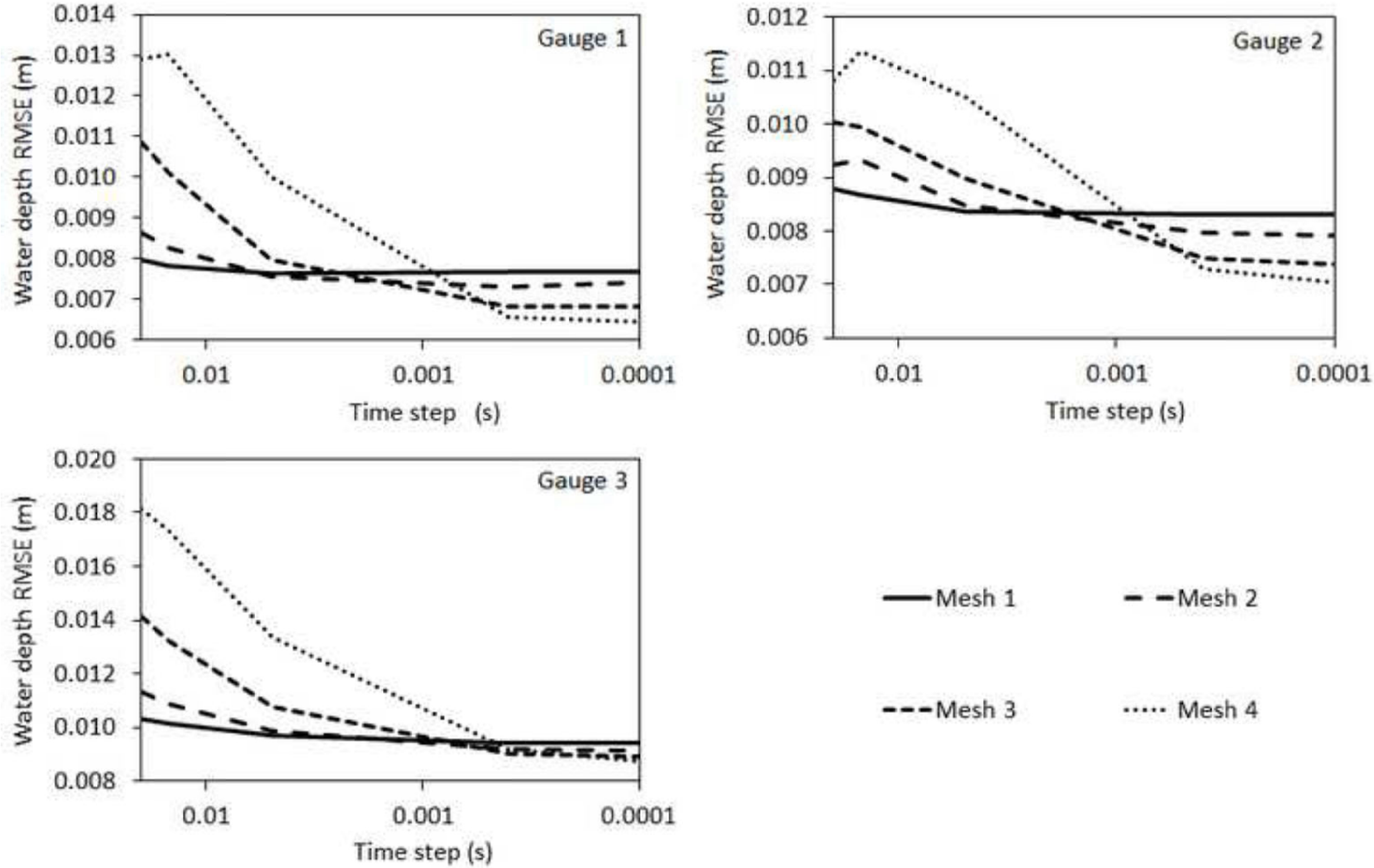
Gauge 1
Water depth RMSE (m)
0.014
0.013
0.012
0.011
0.010
0.009
0.008
0.007
0.006
0.01
0.001
0.0001
Time step (s)
Gauge 2
Water depth RMSE (m)
0.012
0.011
0.010
0.009
0.008
0.007
0.006
0.01
0.001
0.0001
Time step (s)
Gauge 3
Water depth RMSE (m)
0.020
0.018
0.016
0.014
0.012
0.010
0.008
0.01
0.001
0.0001
Time step (s)
Mesh 1
Mesh 2
Mesh 3
Mesh 4

Figure 5



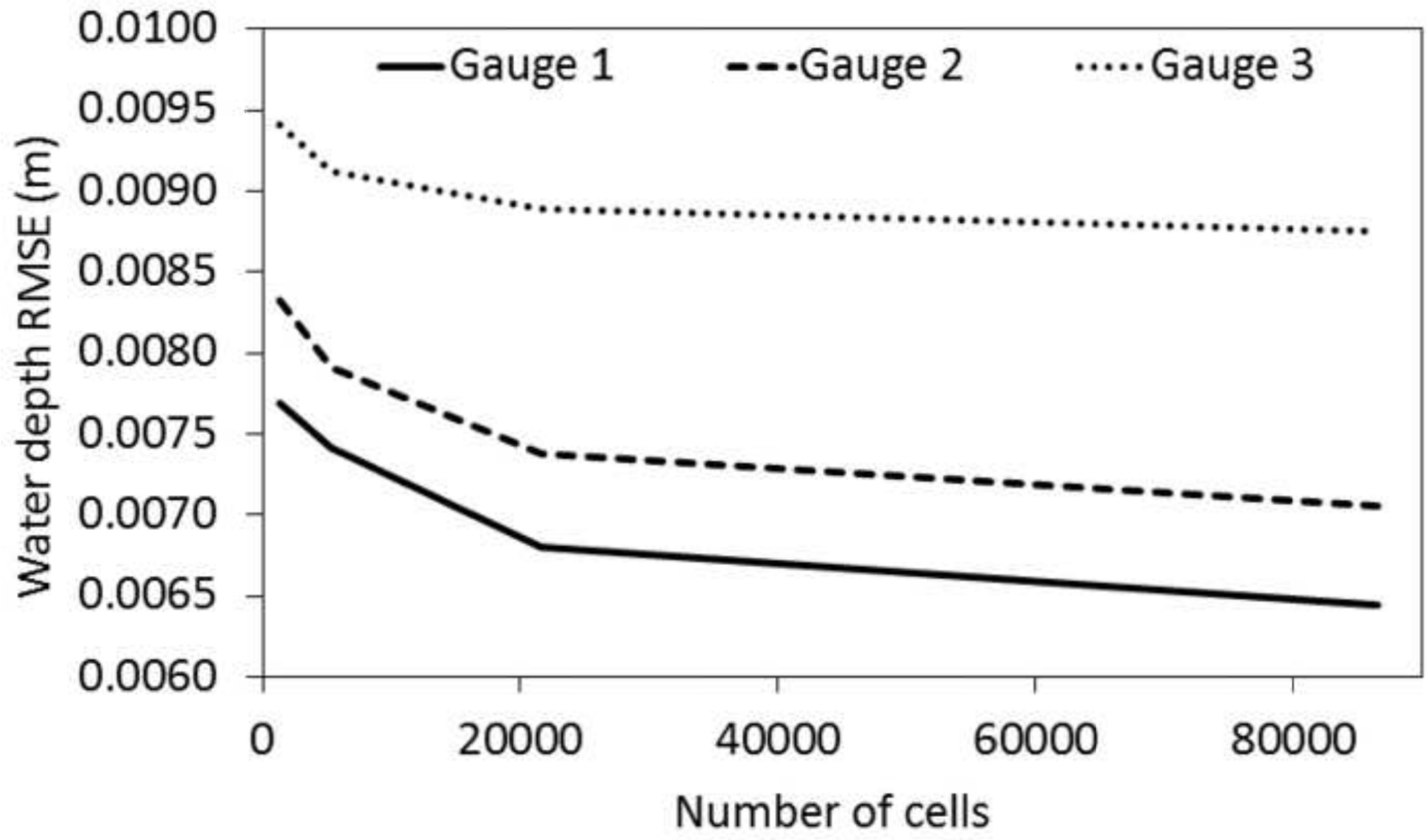
Gauge 1
Gauge 2
Gauge 3
Water depth RMSE (m)
0.0100
0.0095
0.0090
0.0085
0.0080
0.0075
0.0070
0.0065
0.0060
0
20000
40000
60000
80000
Number of cells

Figure 6



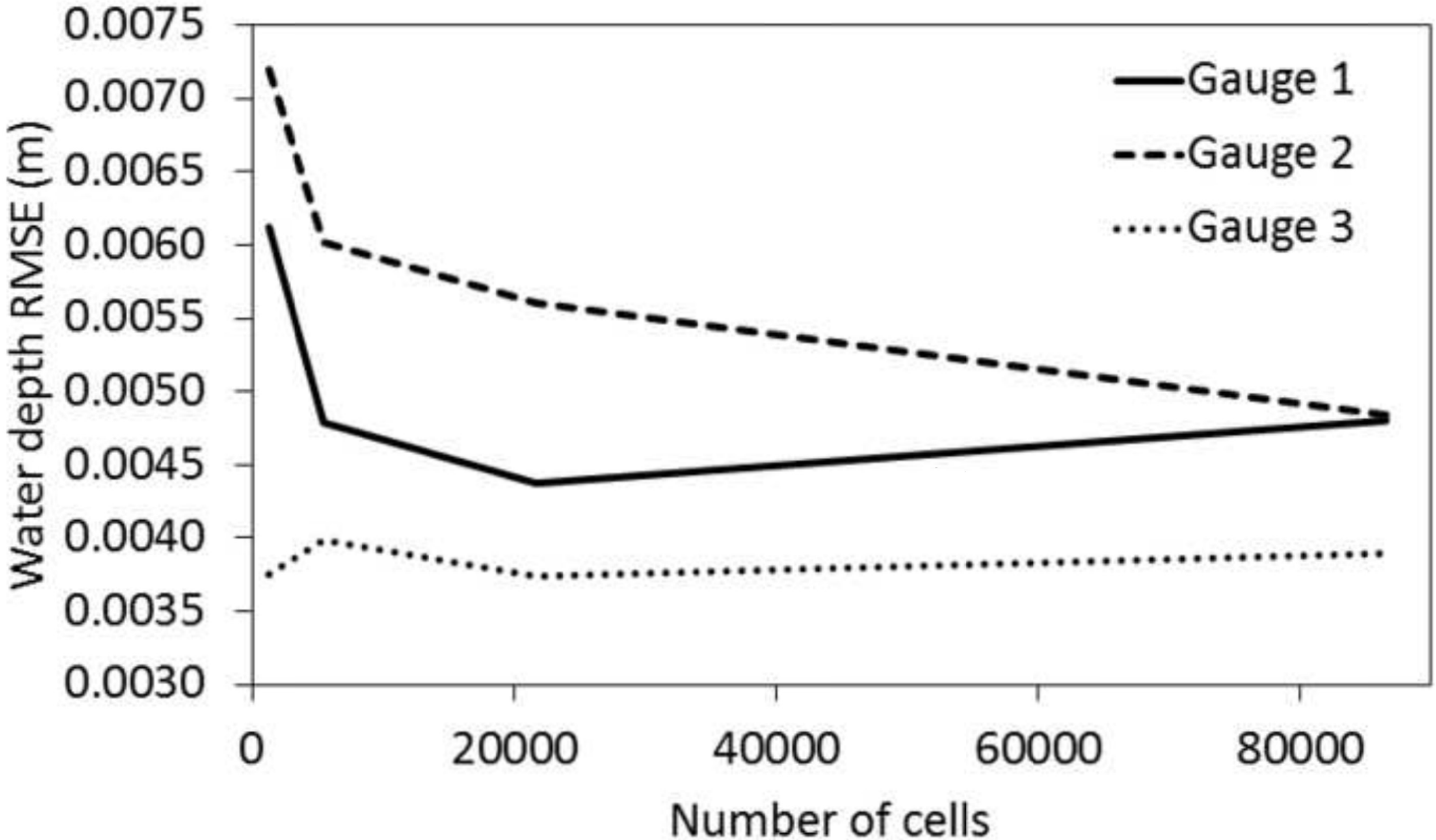
Gauge 1
Gauge 2
Gauge 3
0.0075
0.0070
0.0065
0.0060
0.0055
0.0050
0.0045
0.0040
0.0035
0.0030
Water depth RMSE (m)
0
20000
40000
60000
80000
Number of cells

Figure 7



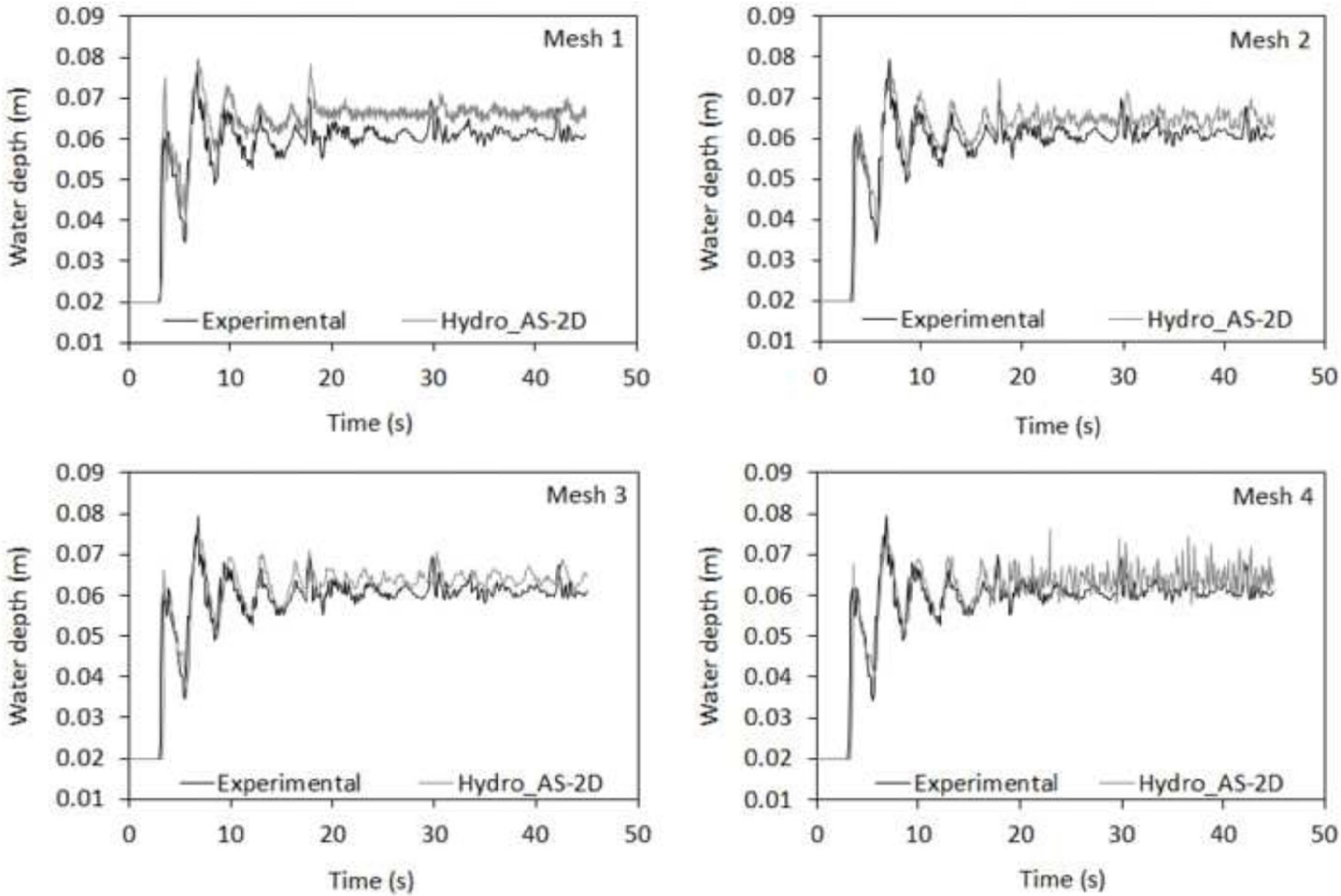
Mesh 1
Mesh 2
Mesh 3
Mesh 4
Water depth (m)
Time (s)
0.09
0.08
0.07
0.06
0.05
0.04
0.03
0.02
0.01
0
10
20
30
40
50
Experimental
Hydro_AS-2D

Figure 8



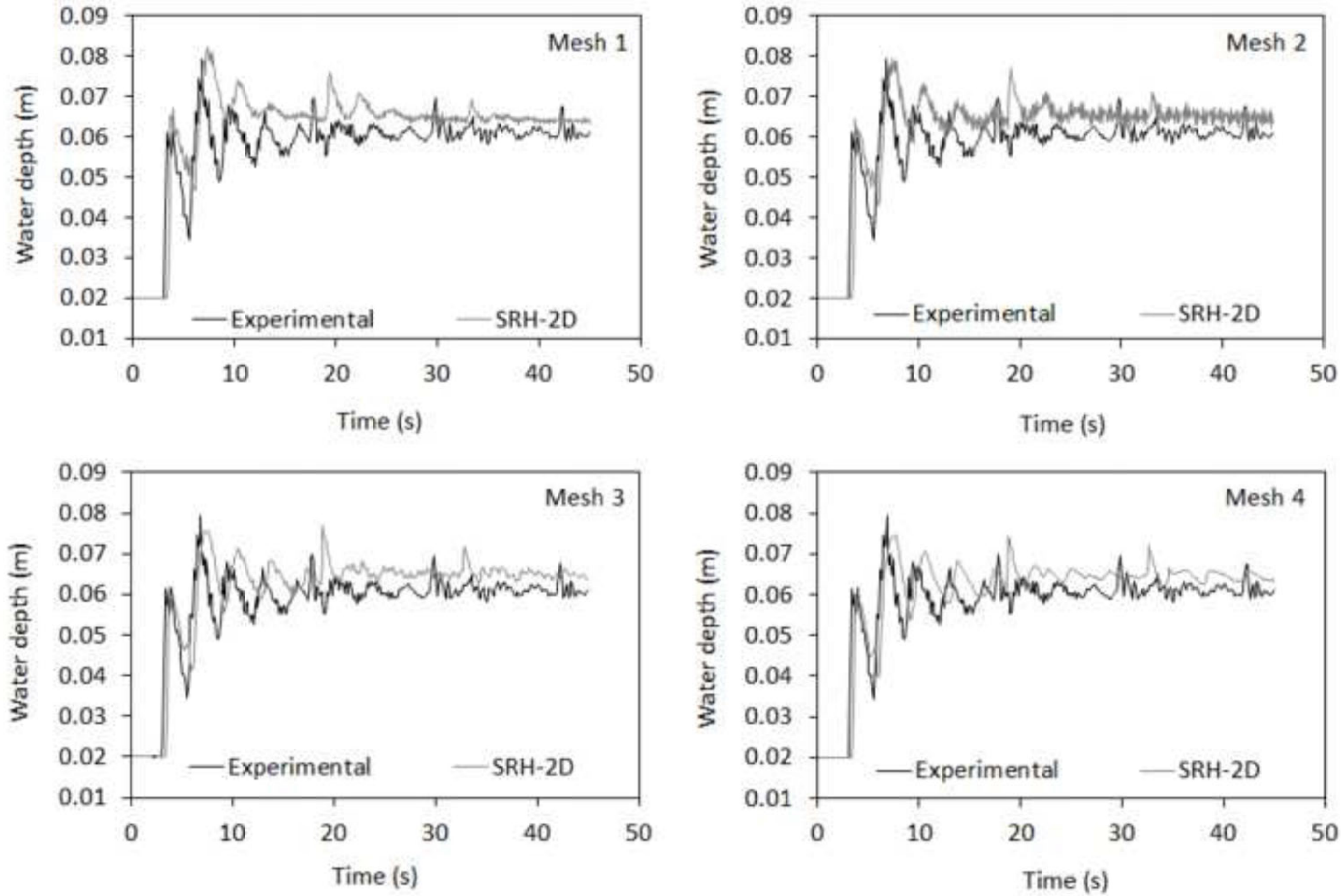
Mesh 1
Mesh 2
Mesh 3
Mesh 4
Water depth (m)
Time (s)
Experimental
SRH-2D
0.09
0.08
0.07
0.06
0.05
0.04
0.03
0.02
0.01
0
10
20
30
40
50

Figure 9



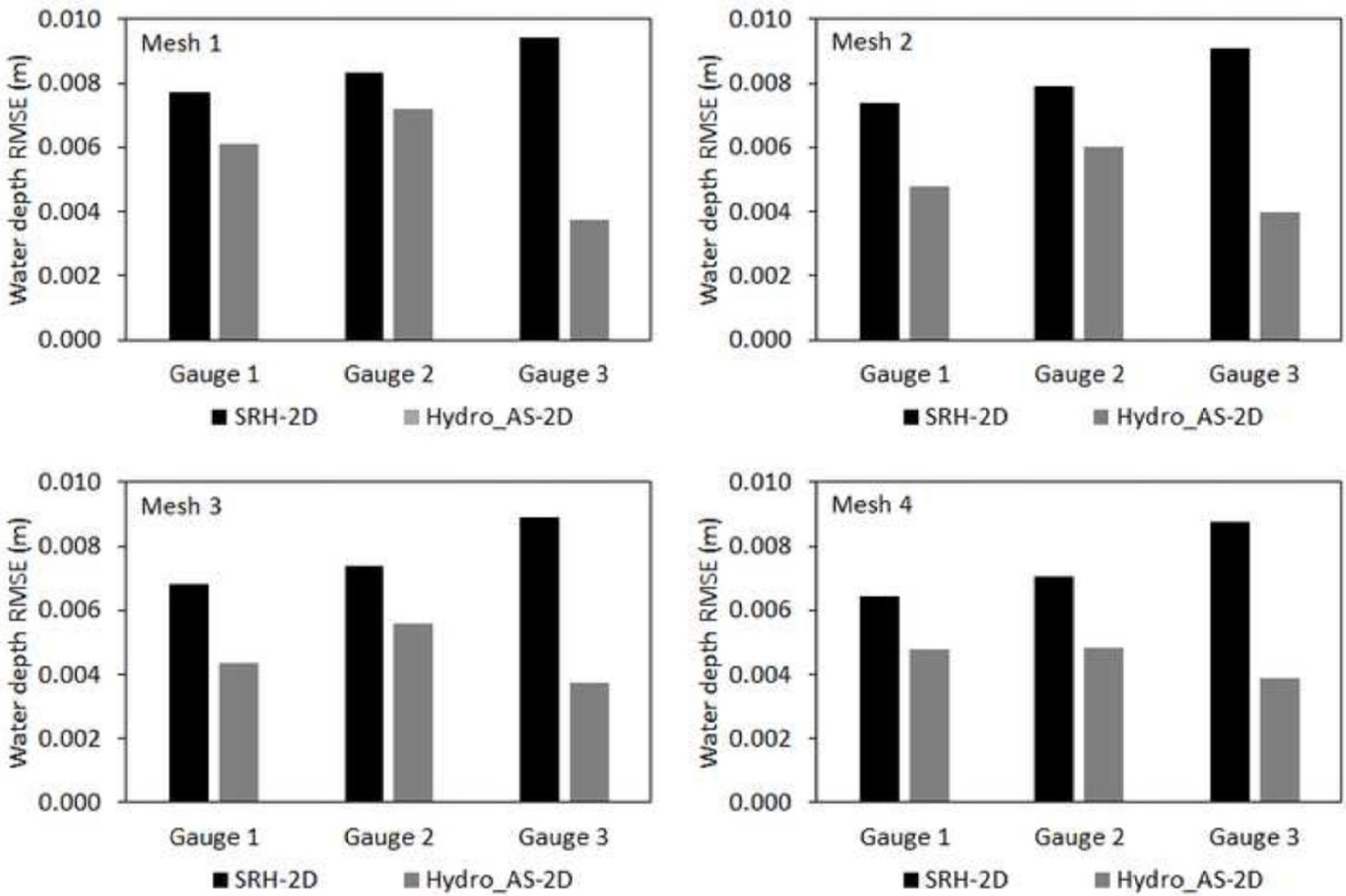
Mesh 1
Mesh 2
Mesh 3
Mesh 4
Water depth RMSE (m)
0.010
0.008
0.006
0.004
0.002
0.000
Gauge 1
Gauge 2
Gauge 3
SRH-2D
Hydro_AS-2D

Figure 10



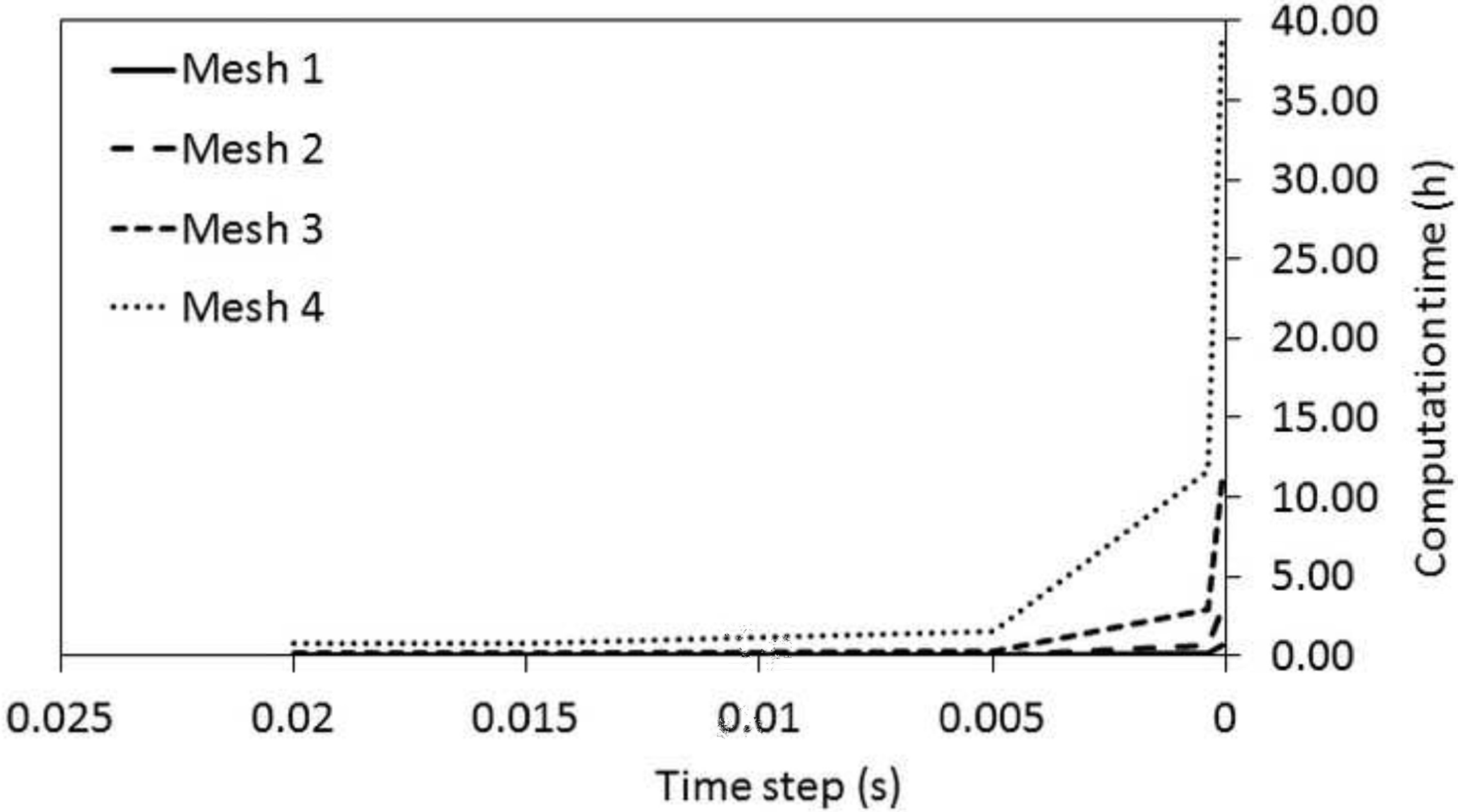

Mesh 1
Mesh 2
Mesh 3
Mesh 4
40.00
35.00
30.00
25.00
20.00
15.00
10.00
5.00
0.00
Computation time (h)
0.025
0.02
0.015
0.01
0.005
0
Time step (s)

Figure 11



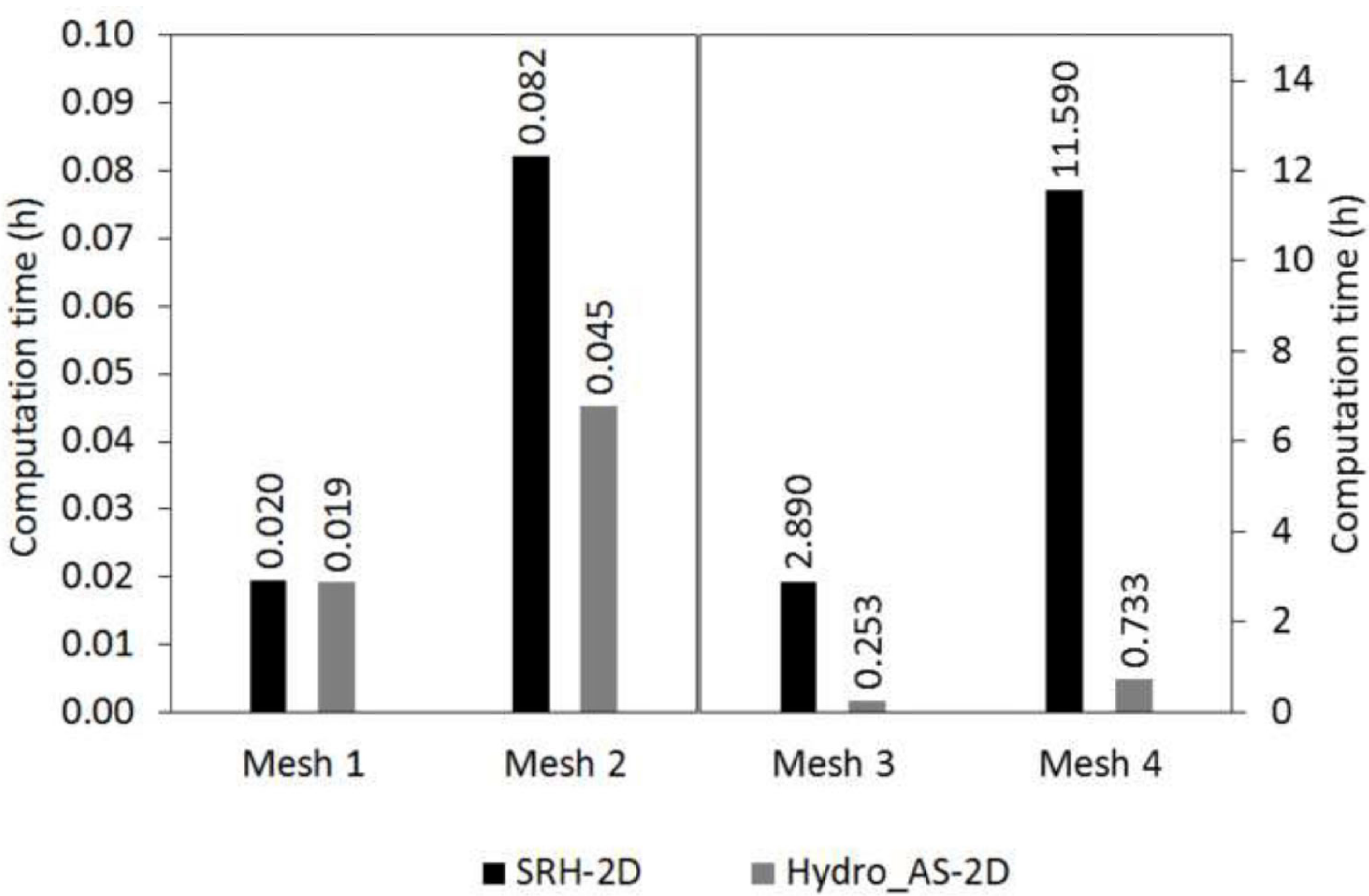

Computation time (h)
0.10
0.09
0.08
0.07
0.06
0.05
0.04
0.03
0.02
0.01
0.00
0.020
0.019
0.082
0.045
2.890
0.253
11.590
0.733
14
12
10
8
6
4
2
0
Computation time (h)
Mesh 1
Mesh 2
Mesh 3
Mesh 4
SRH-2D
Hydro_AS-2D

Figure 12



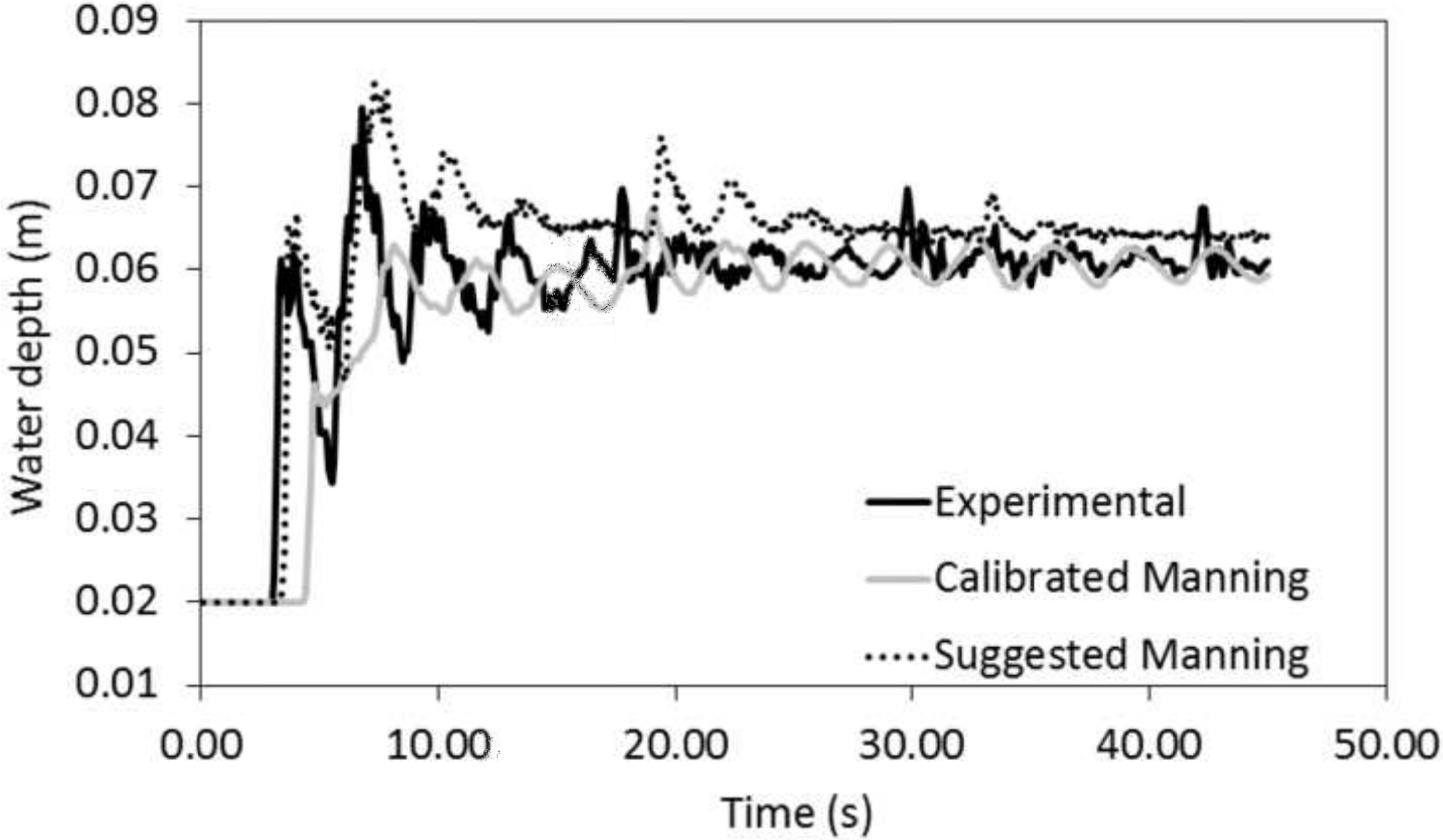
0.09
0.08
0.07
0.06
0.05
0.04
0.03
0.02
0.01
Water depth (m)
0.00
10.00
20.00
30.00
40.00
50.00
Time (s)
Experimental
Calibrated Manning
Suggested Manning

**Table 1.** Time steps

| ID | Time Step (s) |
|---|---|
| 1 | 0.02 |
| 2 | 0.015 |
| 3 | 0.005 |
| 4 | 0.0004 |
| 5 | 0.0001 |

**Table 2.** Cells' number for the different meshes

| ID | Number of Cells |
|---|---|
| 1 | 1 353 |
| 2 | 5 412 |
| 3 | 21 648 |
| 4 | 86 592 |

 

**Table 3.** Time steps used for computation time comparison

| | SRH-2D (s) | Hydro_AS-2D (s) |
|---|---|---|
| Mesh 1 | 0.005 | 0.020691 |
| Mesh 2 | 0.005 | 0.001282 |
| Mesh 3 | 0.0004 | 0.001675 |
| Mesh 4 | 0.0004 | 0.000369 |

**Table 4.** Calibration parameters and results

| | SRH-2D | | Hydro_AS-2D | |
|---|---|---|---|---|
| | Calibrated n | Suggested n | Calibrated n | Suggested n |
| RMSE Gauge 1 (m) | 0.00821 | 0.00765 | 0.00640 | 0.00613 |
| RMSE Gauge 2 (m) | 0.00518 | 0.00837 | 0.00739 | 0.00720 |
| RMSE Gauge 3 (m) | 0.00754 | 0.00972 | 0.00403 | 0.00375 |
| Model calls | 38 | | 19 | |
| Iterations | 10 | | 3 | |
| Calibrated n ($s/m^{1/3}$) | 0.0219 | | 0.0096 | |
| Suggested n ($s/m^{1/3}$) | 0.011 | | 0.011 | |
| Computation time (h) | 1.08 | | 1.2 | |